ELSEVIER

International Journal of Solids and Structures 41 (2004) 4337–4347

INTERNATIONAL JOURNAL OF SOLIDS and STRUCTURES

www.elsevier.com/locate/ijsolstr

An electrical field based non-linear model in the fracture of piezoelectric ceramics

B.L. Wang [a], X.H. Zhang [b,*]

[a] *Department of Manufacturing Engineering and Engineering Management (MEEM), City University of Hong Kong, 83 Tat Chee Avenue, Kowloon, Hong Kong, PR China*

[b] *Centre for Advanced Materials Technology (CAMT), School of Aerospace, Mechanical and Mechatronic Engineering J07, The University of Sydney, Sydney, NSW 2006, Australia*

Received 11 January 2004; received in revised form 11 January 2004
Available online 16 April 2004

Abstract

An analytical model based upon electric field saturation concept along the crack front is proposed in an attempt to predict the fracture of piezoelectric materials containing conducting cracks. Firstly, linear piezoelectroelasticity solution is obtained to show the singularity of the electric field near the crack tips. Then an electrically yielding strip near the crack front is proposed. Expressions for the stress intensity factor K and the energy release rate G are obtained in closed-form. Fracture criteria based on the non-linear fracture mechanics parameters K and G are established, which are shown to be equivalent for some special situations. Theoretically predicated fracture loads agree qualitatively with existing experimental observations.

1. Introduction

Piezoelectric effect occurs in a number of ceramics. The direct piezoelectric effect relates a change in the polarization to an applied stress, whereas the converse effect relates a dimensional change to an applied electric field. Piezoelectric ceramic materials are very brittle and have low strength. Hence, reliability studies have to be performed. In particular, it is necessary to understand the influence of electric fields on the fracture strength of piezoelectric materials. Experiments have shown that crack growth under electrical or electromechanical loads is responsible for failure of many electroceramic systems. Some years ago, Suo et al. (1992) expanded the fracture mechanical concept to piezoelectric materials. Among various fracture modes, dielectric breakdown associated with the growth of conducting cracks has received considerable attention (Suo, 1993; Winzer et al., 1989; Zeller and Schneider, 1984). Recently, several important issues regarding the effect of electric fields on crack growth in piezoelectric materials have been reported in the

* Corresponding author.
E-mail addresses: wangbl2001@hotmail.com, baolin.wang@aeromech.usyd.edu.au (B.L. Wang), xinghong.zhang@aeromech.usyd.edu.au (X.H. Zhang).

0020-7683/$ - see front matter © 2004 Elsevier Ltd. All rights reserved.
doi:10.1016/j.ijsolstr.2004.01.027

literature. Insulating and conducting cracks are two main assumptions, which have been widely used to study the fracture behavior of piezoelectric ceramics. Analysis based on a linear piezoelectric model predicts that an electric field does not produce any stress intensity factor and positive driving force for an insulating crack. However, experimental observations suggested that crack growth can be enhanced or retarded by electric field (Park and Sun, 1995; Heyer et al., 1998; Zhang et al., 2003). In order to explain experimental observations, a simplified model of perfect electrical displacement saturation has been applied to insulating cracks in piezoelectric materials (Fulton and Gao, 1997; Gao et al., 1997; Ru, 1999; Wang, 2000). In such an electrical displacement saturation model, the region near the crack front is assumed to yield electrically to reach an electric displacement saturation limit. Besides the electric displacement saturation model, the ferroelectric/ferroelastic process zone models can also describe the observed experiment phenomena quite well (Yang and Zhu, 1998; Ricoeur and Kuna, 2003).

On the other hand, when the applied electric field in a solid dielectric increases up to an upper limit, the dielectric will be electrically breakdown (Kuffel and Zaengl, 1984). Electrical breakdown is a common phenomenon in solid dielectrics under high electric field. The breakdown strength E_c is a property of the material and temperature. The values required for an intrinsic breakdown are well in excess of 10^6 V/cm for an idea dielectric without any defects. The electrical breakdown in general is accomplished through the formulation of discharge channels. In fact, a tree-like pattern discharge near the tip of an electrode (where the electric field singularity exists) has been observed (Cooper, 1963). The tree-like pattern discharge was also observed in dielectric failure where non-uniform electric field predominate (Kuffel and Zaengl, 1984).

Based on the above facts, we proposed an electrical field saturation model in this paper. That is, we consider an electrical field saturation strip around the crack tip. The model is analogous to the "electrical displacement saturation model" and is referred to as "electrical field saturation model" in this paper. We only consider the interior crack problem, which provides a useful analog to the more important surface/edge crack problem. Closed-form solution for this model has been obtained and some calculations results for the fracture predictions are given.

2. Basic piezoelectric elasticity equations

We investigate the plane problem of the infinite piezoelectric medium shown in Fig. 1. Assume that all field variables are functions of x_1 and x_2 only. The coordinates x and y coincide with x_1 and x_2 respectively. Constitutive equations for piezoelectric materials polarized along the x_1-direction subjected to mechanical and electrical fields can be written as

$$\begin{Bmatrix} \sigma_{22} \\ \sigma_{11} \\ \sigma_{12} \\ D_2 \\ D_1 \end{Bmatrix} = \begin{bmatrix} c_{11} & c_{13} & 0 & 0 & -e_{31} \\ c_{13} & c_{33} & 0 & 0 & -e_{33} \\ 0 & 0 & c_{44} & -e_{15} & 0 \\ 0 & 0 & e_{15} & \in_{11} & 0 \\ e_{31} & e_{33} & 0 & 0 & \in_{33} \end{bmatrix} \begin{Bmatrix} \varepsilon_{22} \\ \varepsilon_{11} \\ 2\varepsilon_{12} \\ E_2 \\ E_1 \end{Bmatrix}. \tag{1}$$

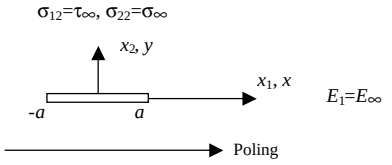

Fig. 1. A piezoelectric medium with a through-thickness conducting crack.

where σ_{ij} and D_i are stresses and electric displacements, respectively; c_{ij}, e_{ij}, and $\in_{ii}$ are elastic constants, piezoelectric constants, and dielectric permittivities, respectively. The strain, ε_{ij} is related to the mechanical displacement, u_i, as $\varepsilon_{ij} = (u_{i,j} + u_{j,i})/2$, where a comma indicates a partial derivative. The electric field, E_i is related to the electric potential, ϕ, as $E_i = -\phi_{,i}$.

In order to facilitate the analysis procedure, the constitutive equation (1) is re-written as

$$\begin{Bmatrix} \sigma_{22} \\ \sigma_{11} \\ \sigma_{12} \\ E_2 \\ E_1 \end{Bmatrix} = \begin{bmatrix} \bar{c}_{11} & \bar{c}_{13} & 0 & 0 & \bar{e}_{31} \\ \bar{c}_{13} & \bar{c}_{33} & 0 & 0 & \bar{e}_{33} \\ 0 & 0 & \bar{c}_{44} & \bar{e}_{15} & 0 \\ 0 & 0 & \bar{e}_{15} & \overline{\in}_{11} & 0 \\ \bar{e}_{31} & e_{33} & 0 & 0 & \overline{\in}_{33} \end{bmatrix} \begin{Bmatrix} \varepsilon_{22} \\ \varepsilon_{11} \\ 2\varepsilon_{12} \\ D_2 \\ D_1 \end{Bmatrix}. \tag{2}$$

Since the electric displacement $\boldsymbol{D}$ is divergence-free in the absence of space charge, a potential function $\Phi(x, y)$ exists, giving

$$D_1 = \Phi_{,2}, \quad D_2 = -\Phi_{,1}. \tag{3}$$

It follows from $E_i = \phi_{,i}$ that

$$E_{1,2} - E_{2,1} = 0. \tag{4}$$

The governing equations can be written in terms of displacements u_1 and u_2 and the potential function Φ by inserting Eq. (2) into Eq. (4) and the mechanical equilibrium conditions $\sigma_{ji,j} = 0$, giving:

$$\left.\begin{array}{l} \bar{c}_{33}u_{1,11} + \bar{c}_{44}u_{1,22} + (\bar{c}_{13} + \bar{c}_{44})u_{2,12} + (\bar{e}_{33} - \bar{e}_{15})\Phi_{,12} = 0 \\ (\bar{c}_{13} + \bar{c}_{44})u_{1,12} + \bar{c}_{44}u_{2,11} + \bar{c}_{11}u_{2,22} - \bar{e}_{15}\Phi_{,11} + \bar{e}_{31}\Phi_{,22} = 0 \\ (\bar{e}_{33} - \bar{e}_{15})u_{1,12} + \bar{e}_{31}u_{2,22} - \bar{e}_{15}u_{2,11} + \overline{\in}_{33}\Phi_{,22} + \overline{\in}_{11}\Phi_{,11} = 0 \end{array}\right\}. \tag{5}$$

3. The linear piezoelectric crack problem

Fig. 1 shows a piezoelectric medium with a crack of length $2a$ along the x_1-axis. Let the piezoelectric medium be loaded by a remote uniform shear stress τ_∞, a normal stress σ_∞ in the x_2-direction and an electric field E_∞ in the x_1-direction. The crack is electrically conducting and free of mechanical forces. Therefore, the crack surface conditions can be stated as follows

$$\sigma_{21} = 0, \quad \sigma_{22} = 0, \quad E_1(x, 0) = 0, \qquad |x| < a. \tag{6}$$

In the following analysis, we will use the following notations

$$\{b\} = \{b_1, b_2, b_3\}^{\mathrm{T}} = \{\sigma_{12}, \sigma_{22}, E_1\}^{\mathrm{T}}, \tag{7a}$$

$$\{b^\infty\} = \{b_1^\infty, b_2^\infty, b_3^\infty\}^{\mathrm{T}} = \{\tau_\infty, \sigma_\infty, E_\infty\}^{\mathrm{T}}, \tag{7b}$$

$$\{U\} = \{U_1, U_2, U_3\}^{\mathrm{T}} = \{u_1, u_2, \Phi\}^{\mathrm{T}}, \tag{7c}$$

The solution technique employed in the following is not new. There are enormous references related to this technique. The displacements and the potential function Φ will be derived from Fourier integrals and characteristic equations. The boundary conditions on the crack surfaces are satisfied by some auxiliary functions. A system of singular integral equations is finally derived and the crack tip field is then obtained.

Analog to the solution of crack problems for orthotropic elasticity (e.g., Konda and Erdogan, 1994), the solution of Eq. (5) can be expressed as:

$$U_J(x_1,x_2)=\frac{1}{2\pi}\int_{-\infty}^{\infty}\exp(|s|\lambda_m x_2)A_{Jm}\exp(-\mathrm{i}sx_1)F_m\,\mathrm{d}s+f_J(x_1,x_2), \tag{8}$$

where f_J ($J=1,2,3$) are particular solutions determined from the far-field boundary conditions; the first term on the right-hand side of Eq. (8) is the general solution of Eq. (5) which should vanish at infinity; $F_m(s)$ are unknown functions; λ_m are eigenvalues, (A_{1m},A_{2m},A_{3m}) are corresponding eigenvectors of the following characteristic equations

$$\begin{bmatrix} \bar{c}_{33}-\bar{c}_{44}\lambda_m^2 & \mathrm{isgn}\,(s)(\bar{c}_{13}+\bar{c}_{44})\lambda_m & \mathrm{isgn}\,(s)(\bar{e}_{33}-\bar{e}_{15})\lambda_m \\ \mathrm{isgn}\,(s)(\bar{c}_{13}+\bar{c}_{44})\lambda_m & \bar{c}_{44}-\bar{c}_{11}\lambda_m^2 & -\bar{e}_{15}-\bar{e}_{31}\lambda_m^2 \\ \mathrm{isgn}\,(s)(\bar{e}_{33}-\bar{e}_{15})\lambda_m & -\bar{e}_{15}-\bar{e}_{31}\lambda_m^2 & \overline{\in}_{11}-\overline{\in}_{33}\lambda_m^2 \end{bmatrix}\begin{Bmatrix} A_{1m} \\ A_{2m} \\ A_{3m} \end{Bmatrix}=0. \tag{9}$$

Since the stress and electric fields given by the infinite integral on the right-hand side of Eq. (8) must vanish as x_2 approaches infinity, only those eigenvalues of Eq. (9) involve negative real parts for $x_2>0$ and positive real parts for $x_2<0$ should be considered.

The stress and electrical fields can be obtained by differentiating Eq. (8) to obtain the strain and electric displacement fields, and substituting the strain and electrical displacement fields into the electroelastic constitutive equations (2). This gives:

$$b_J=\frac{1}{2\pi}\int_{-\infty}^{\infty}s\exp(|s|\lambda_m x_2)C_{Jm}\exp(-\mathrm{i}sx_1)F_m\,\mathrm{d}s+b_J^{\infty}, \tag{10}$$

where $C_{Jm}(s)$, ($J=1,2,3$), are some coefficients which depend only on material properties.

To satisfy boundary conditions (6) on crack surfaces, we again analog to the solution of crack problems for orthotropic elasticity (e.g., Konda and Erdogan, 1994). That is we introduce an auxiliary vector $\{g(x)\}=\{g_1(x),g_2(x),g_3(x)\}^{\mathrm{T}}$ along the crack plane

$$g_J=\frac{\partial U_J(x_1,+0)}{\partial x_1}-\frac{\partial U_J(x_1,-0)}{\partial x_1}. \tag{11}$$

From the continuity conditions on the $x_2=0$ plane, it can be shown that $\{g(x)\}$ vanishes for $|x_1|>a$. Substituting of Eq. (8) into Eq. (11) leads to the expressions for F_m, in terms of the Fourier transform of $\{g(x)\}$. Those expressions are substituting into Eq. (10) to obtain the stress and electric fields $\{b(x_1,x_2)\}$, in terms of $\{g(x)\}$. On the $x_2=0$ plane, we have:

$$\{b(x,0)\}=\frac{[\Lambda]}{\pi}\int_{-a}^{a}\frac{1}{r-x}\{g(r)\}\,\mathrm{d}r+\{b^{\infty}\}, \tag{12}$$

in which $[\Lambda]$ is a (3×3) matrix which depends only on material properties. It follows from Eq. (12) and boundary conditions (6) that

$$\frac{[\Lambda]}{\pi}\int_{-a}^{a}\frac{1}{r-x}\{g(r)\}\,\mathrm{d}r=-\{b^{\infty}\},\quad |x|<a. \tag{13}$$

Eq. (13) can be directly inverted to yield

$$\{g(x)\}=-[\Lambda^{-1}]\{b^{\infty}\}\frac{x}{\sqrt{a^2-x^2}},\quad |x|<a, \tag{14}$$

where $[\Lambda^{-1}]$ is the inversion of matrix $[\Lambda]$.

Since the crack is electrically conducting, the electrical potential on its surfaces is a constant. However, the charges will accumulate on the crack surfaces. According to Eq. (11), the crack sliding displacements Δu_1 and opening displacement Δu_2 across the crack, and the accumulated charge Δq on the crack surfaces, can be obtained by integrating Eq. (14), giving

$$\{\Delta u_1(x), \Delta u_2(x), \Delta q(x)\}^{\mathrm{T}} = [\Lambda^{-1}]\{b^{\infty}\}\sqrt{a^2 - x^2}, \quad |x| < a, \tag{15}$$

where $\Delta u_i(x)$, $(i = 1, 2)$ are displacement differences between the upper and lower surfaces of the crack, $\Delta q(x)$ is the sum of the accumulated charges on the upper and lower surfaces of the crack. $\Delta q(x)$ has a unit of charge per unit length.

In order to derive the stress and electric fields near the crack tips, we use Eq. (14) to derive the expression:

$$\frac{[\Lambda]}{\pi}\int_{-a}^{a}\frac{1}{r-x}\{g(r)\}\,\mathrm{d}r = \{b^{\infty}\}\mathrm{Re}\left(\frac{|x|}{\sqrt{x^2-a^2}} - 1\right). \tag{16}$$

Substituting it into Eq. (12), we obtain

$$\{b\} = \{b^{\infty}\}\mathrm{Re}\left(\frac{|x|}{\sqrt{x^2-a^2}}\right). \tag{17}$$

Eq. (17) shows that ahead of the crack tips, the stress and electric fields are singular. From Eq. (17) together with the definition of the stress and electric field intensity factors:

$$\begin{aligned} &K_{\mathrm{II}} = \lim_{x\to a+0}\sigma_{21}(x,0)\sqrt{2\pi(x-a)}, \quad K_{\mathrm{I}} = \lim_{x\to a+0}\sigma_{22}(x,0)\sqrt{2\pi(x-a)},\\ &K_{\mathrm{E}} = \lim_{x\to a+0}E_1(x,0)\sqrt{2\pi(x-a)}, \end{aligned} \tag{18}$$

we obtain

$$K_{\mathrm{I}} = \sigma_{\infty}\sqrt{\pi a}, \quad K_{\mathrm{II}} = \tau_{\infty}\sqrt{\pi a}, \quad K_{\mathrm{E}} = E_{\infty}\sqrt{\pi a}. \tag{19}$$

where K_{I} and K_{II} are, respectively, modes I and II stress intensity factors, K_{E} is the electric field intensity factor. They are defined in Eq. (18).

The energy release rate can be obtained from the virtual crack closure integral:

$$G = \frac{1}{2}\lim_{\delta\to 0}\int_0^{\delta}[\sigma_{2j}(x+a)\Delta u_j(x+a-\delta) + E_1(x+a)\Delta q(x+a-\delta)]\,\mathrm{d}x, \quad j = 1, 2. \tag{20}$$

Here and in the sequel the summation over the indices i, j, I and J is assumed $(i, j = 1, 2;\ I, J = 1, 2, 3)$. Substituting of Eqs. (15) and (17) into Eq. (20) leads to

$$G = \frac{\pi a}{4}b_I^{\infty}\Lambda_{IJ}^{-1}b_J^{\infty}, \quad I, J = 1, 2, 3, \tag{21}$$

or

$$G = \frac{1}{4}\{K_{\mathrm{II}}, K_{\mathrm{I}}, K_{\mathrm{E}}\}[\Lambda^{-1}]\{K_{\mathrm{II}}, K_{\mathrm{I}}, K_{\mathrm{E}}\}^{\mathrm{T}}. \tag{22}$$

In Eq. (21) and in the following, Λ_{IJ}^{-1} $(I, J = 1, 2, 3)$ are the elements in matrix $[\Lambda^{-1}]$. For stable materials, the matrix $[\Lambda]$ should be positive defined. Therefore, G is a positive defined function of the applied stress and electric fields. Hence, G increases as the strength of the applied electric field increases either in positive or in negative directions. This fact suggests that if linear fracture mechanics parameter G is used as a fracture criterion, the existence of an electric field may enhance crack propagation regardless of its direction.

4. An electrical field saturation model

Consider again a piezoelectric medium with a crack of length $2a$ along the x-axis. Let the medium be loaded by remote uniform normal stresses τ_∞ and σ_∞ in the x_2-direction and a uniform electric field E_∞ in the x_1-axis. Electrically, the crack is considered as a conductor. For such a crack configuration, the above linear piezoelectric analysis shows that the electric fields at the crack tips is singular. It is expected that the electric field near the crack tips is high enough to reach a limit value so that the medium near the crack tip region is electrically yielding.

Analogous to the electrical displacement saturation model proposed by Fulton and Gao (1997) and Gao et al. (1997), the above problem can be highly simplified to a conducting crack with an electric field saturation strip $a < |x| < c$ ahead of the crack tips, as shown in Fig. 2 (Zhang and Gao, 2004). The saturation region can be modeled as an applied constant electrical field $E_1(x_1) = E_c$ which is defined as a fraction of the electrical breakdown strength of the medium. This condition is equivalent to the singular integral equations:

$$\frac{\Lambda_{iJ}}{\pi}\int_{-c}^{c}\frac{1}{r-x}g_J(r)\,\mathrm{d}r = -b_i^{\infty}, \quad |x| < a, \tag{23a}$$

$$\frac{\Lambda_{3J}}{\pi}\int_{-c}^{c}\frac{1}{r-x}g_J(r)\,\mathrm{d}r = p(x) - b_3^{\infty}, \quad |x| < c. \tag{23b}$$

where $i = 1, 2$ and $J = 1, 2, 3$. The electric field saturation function $p(x)$ is defined as

$$p(x) = \begin{cases} 0 & \text{if } |x| < a \\ E_c & \text{if } c > |x| > a. \end{cases} \tag{24}$$

4.1. Stress intensity factor

Mechanically, the crack is closed at $|x| = a$. Therefore, the auxiliary functions g_1 and g_2 vanish for $|x| \geqslant a$. Eqs. (23) can be directly solved to give

$$g_i(x) = -\Lambda_{iJ}^{-1}b_J^{\infty}\frac{x}{\sqrt{a^2-x^2}}, \quad |x| < a, \ \ i = 1,2. \tag{25}$$

In order to derive the stress and electric fields ahead of the crack tips, we use Eqs. (25) and (23b) to derive the expressions:

$$\int_{-a}^{a}\frac{1}{r-x}g_i(r)\,\mathrm{d}r = \pi\Lambda_{iJ}^{-1}b_J^{\infty}\mathrm{Re}\left(\frac{|x|}{\sqrt{x^2-a^2}} - 1\right), \quad i = 1,2. \tag{26a}$$

$$\int_{-c}^{c}\frac{1}{r-x}g_3(r)\,\mathrm{d}r = \frac{\pi}{\Lambda_{33}}[p(x) - b_3^{\infty}] - \frac{\Lambda_{3i}}{\Lambda_{33}}\int_{-c}^{c}\frac{1}{r-x}g_i(r)\,\mathrm{d}r, \quad |x| < c. \tag{26b}$$

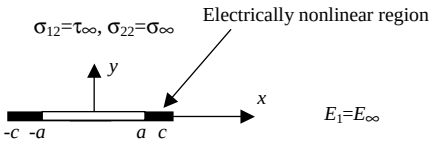

Fig. 2. Electric field saturation model.

Substituting these into the definition Eq. (12), we obtain

$$\sigma_{2i}(x,0) = \left(b_i^{\infty} - \frac{\Lambda_{i3}}{\Lambda_{33}} b_3^{\infty}\right) \mathrm{Re}\left(\frac{|x|}{\sqrt{x^2 - a^2}}\right) + \frac{\Lambda_{i3}}{\Lambda_{33}} p(x), \quad i = 1, 2, \tag{27a}$$

$$E_1(x,0) = p(x), \tag{27b}$$

Eq. (27a) shows that the electric field alone can cause stresses in the cracked plane ahead of the crack tips. This character is quite different from the result of the linear piezoelectric elasticity (see Eq. (17)). Further, ahead of the crack tips, the electric field is finite but the stresses have singularities. From Eq. (27a) together with the definition of the stress intensity factors we obtain

$$K_{\mathrm{II}} = \left(b_1^{\infty} - \frac{\Lambda_{13}}{\Lambda_{33}} b_3^{\infty}\right)\sqrt{\pi a}, \quad K_{\mathrm{I}} = \left(b_2^{\infty} - \frac{\Lambda_{23}}{\Lambda_{33}} b_3^{\infty}\right)\sqrt{\pi a}. \tag{28}$$

Again, it is found that the electrical field load b_3^{∞} can cause stress singularities at the crack tips.

4.2. Energy release rate

In order to obtain the energy release from virtual crack closure integral we need to know the displacement jumps across the crack and the electric charge accumulated on the crack surfaces. It can be shown from Eq. (25) that the crack sliding and opening displacements are same as in the linear case,

$$\Delta u_i(x) = \Lambda_{iJ}^{-1} b_J^{\infty} \sqrt{a^2 - x^2}, \quad |x| < a, \quad i = 1, 2. \tag{29}$$

Referring to Eq. (23b), to ensure that the electric field E_1 is non-singular at the endpoints $|x| = c$, the following equation must hold (Estrada and Kanwal, 2000)

$$\int_{-c}^{c} \frac{p(x) - b_3^{\infty}}{\sqrt{c^2 - x^2}}\, \mathrm{d}x = 0. \tag{30}$$

Eq. (30) gives the size of the saturation region as a function of the ratio of the applied electric field to the electric field saturation limit E_{c}:

$$\frac{a}{c} = \cos\left(\frac{\pi}{2}\frac{E_{\infty}}{E_{\mathrm{c}}}\right). \tag{31}$$

Then, the non-singular solution of (23b) is (Fulton and Gao, 1997; Gao et al., 1997; Estrada and Kanwal, 2000)

$$\Lambda_{3i} g_i(x) + \Lambda_{33} g_3(x) = -\frac{1}{\pi}\sqrt{c^2 - x^2} \int_{-c}^{c} \frac{p(t) - b_3^{\infty}}{(x - t)\sqrt{c^2 - x^2}}\, \mathrm{d}t = -\frac{E_{\mathrm{c}}}{\pi}[\omega(x,a) - \omega(-x,a)], \tag{32}$$

or

$$g_3(x) = -\frac{1}{\pi}\frac{E_{\mathrm{c}}}{\Lambda_{33}}[\omega(x,a) - \omega(-x,a)] - \frac{\Lambda_{3i}}{\Lambda_{33}} g_i(x), \quad |x| < c, \tag{33}$$

where

$$\omega(x,\alpha) = \cosh^{-1}\left|\frac{c^2 - \alpha^2}{c(\alpha - x)} + \frac{\alpha}{c}\right|, \tag{34}$$

in which $\cosh^{-1}$ represents inverse hyperbolic cosine function.

The accumulated charges exist both in the cracked region ($|x| < a$) and in the electrical saturation zone. Integration of Eq. (33) gives:

$$\Delta q(x) = -\frac{1}{\pi}\frac{E_c}{\Lambda_{33}}[(a-x)\omega(x,a) + (a+x)\omega(-x,a)], \quad |x| < c. \tag{35}$$

Once again, the energy release rate G is obtained from the virtual crack closure integral shown in Eq. (20), giving:

$$G = \frac{\pi a}{4}\left[b_I^{\infty}\Lambda_{IJ}^{-1}b_J^{\infty} - \frac{1}{\Lambda_{33}}(b_3^{\infty})^2\right], \quad I,J = 1,2,3. \tag{36}$$

Substituting $b_1^{\infty} = K_{\mathrm{II}}^{\infty}/\sqrt{a}$, $b_2^{\infty} = K_{\mathrm{I}}^{\infty}/\sqrt{a}$ and $b_3^{\infty} = K_{\mathrm{E}}^{\infty}/\sqrt{a}$ into Eq. (36), G can be written in terms of the applied stress and electric field intensity factors.

4.3. Equivalence of the stress intensity factor and the energy release rate

In the problem under consideration, the poling direction of the medium coincides with the crack line (that is, along the x-axis). It can be shown from the following numerical examples that the material characteristic matrix $[\Lambda]$ has the following form:

$$[\Lambda] = \begin{bmatrix} \Lambda_{11} & 0 & 0 \\ 0 & \Lambda_{22} & \Lambda_{23} \\ 0 & \Lambda_{23} & \Lambda_{33} \end{bmatrix}. \tag{37}$$

It follows from Eqs. (28), (36) and (37) that:

$$K_{\mathrm{II}} = b_1^{\infty}\sqrt{\pi a}, \quad K_{\mathrm{I}} = \left(b_2^{\infty} - \frac{\Lambda_{23}}{\Lambda_{33}}b_3^{\infty}\right)\sqrt{\pi a}. \tag{38}$$

$$G = \frac{\pi a}{4}\left[\Lambda_{22}^{-1}\left(b_2^{\infty} - \frac{\Lambda_{23}}{\Lambda_{33}}b_3^{\infty}\right)^2 + \Lambda_{11}^{-1}(b_1^{\infty})^2\right] = \frac{1}{4}(\Lambda_{22}^{-1}K_{\mathrm{I}}^2 + \Lambda_{11}^{-1}K_{\mathrm{II}}^2). \tag{39}$$

A particular case is that if the applied shear stress is zero (i.e., $K_{\mathrm{II}} = 0$), Eq. (39) becomes:

$$G = \frac{\pi a}{4}\Lambda_{22}^{-1}\left(b_2^{\infty} - \frac{\Lambda_{23}}{\Lambda_{33}}b_3^{\infty}\right)^2 = \frac{1}{4}\Lambda_{22}^{-1}K_{\mathrm{I}}^2. \tag{40}$$

It can be shown from Eqs. (38b) and (40) that, for the electric field based non-linear crack model, fracture criteria based on the stress intensity factor and the energy release rate are equivalent. Therefore, either of K and G can be used as a criterion for conducting cracks in piezoelectric materials.

5. Applications

In order to demonstrate the applicability of the electric field saturation model for the piezoelectricity fracture problem, we evaluate the expressions obtained for two particular materials, namely PZT-4 and PZT-PIC 151. The properties are given in Tables 1–3 (Fulton and Gao, 1997; Heyer et al., 1998). The experimental results for PZT-PIC 151 material are also available (Heyer et al., 1998).

After solving the problem for the poling direction parallel to the x-axis, we obtain the matrices:

$$[\Lambda] = \begin{bmatrix} 2.164 & 0 & 0 \\ 0 & 2.838 & 0.05338 \\ 0 & 0.05338 & 0.005375 \end{bmatrix} \times 10^{10} \quad \text{for PZT-4, and}$$

Table 1
Elastic constants (10^{10} N/m^2)

Materials	c_{11}	c_{12}	c_{13}	c_{44}	c_{33}
PZT-4	13.9	7.78	7.43	2.56	11.3
PZT-PIC 151	11	6.3	6.4	2	10

Table 2
Piezoelectric constants (C/m^2)

Materials	e_{31}	e_{33}	e_{15}
PZT-4	−6.980	13.84	13.44
PZT-PIC 151	−9.6	15.1	12

Table 3
Dielectric permittivities (10^{-10} C/V m)

Materials	$\in_{11}$	$\in_{33}$
PZT-4	60.0	54.7
PZT-PIC 151	98.24	75.4

$$[A] = \begin{bmatrix} 1.743 & 0 & 0 \\ 0 & 2.274 & 0.04047 \\ 0 & 0.04047 & 0.003830 \end{bmatrix} \times 10^{10} \quad \text{for PZT-PIC 151}$$

Here the plane-strain condition is considered. For a crack along the x_1-axis, with loads σ_∞ perpendicular to and E_∞ parallel to the crack line, the stress intensity factor K_{I} and the energy release rate G are obtained as follows:

PZT-4:

$$K_{\mathrm{I}} = \sigma_\infty \sqrt{\pi a}, \quad G = a(0.3403\sigma_\infty^2 - 6.758E_\infty\sigma_\infty + 179.7E_\infty^2) \times 10^{-10}$$

for linear piezoelectric crack, and

$$K_{\mathrm{I}} = (\sigma_\infty - 9.931E_\infty)\sqrt{\pi a}, \quad G = a(0.3403\sigma_\infty^2 - 6.758E_\infty\sigma_\infty + 33.55E_\infty^2) \times 10^{-10}$$

for electrically non-linear crack.

PZT-PIC 151:

$$K_{\mathrm{I}} = \sigma_\infty \sqrt{\pi a}, \quad G = a(0.4254\sigma_\infty^2 - 8.990E_\infty\sigma_\infty + 252.6E_\infty^2) \times 10^{-10}$$

for linear piezoelectric crack, and

$$K_{\mathrm{I}} = (\sigma_\infty - 10.57E_\infty)\sqrt{\pi a}, \quad G = a(0.4254\sigma_\infty^2 - 8.990E_\infty\sigma_\infty + 47.50E_\infty^2) \times 10^{-10}$$

for electrically non-linear crack.

The typical value of the fracture toughness of piezoelectric ceramics in the absence of electric field is around $K_{\mathrm{IC}} = 1$ Mpa $\sqrt{\mathrm{m}}$. Suppose a crack with half-length of $a = 1$ mm, the predicted fracture loads for PZT-PIC 151 are shown in Fig. 3. For comparison, predictions based on linear stress intensity factor and energy release rate are also given. As shown in Eq. (40), there is no difference between the stress intensity

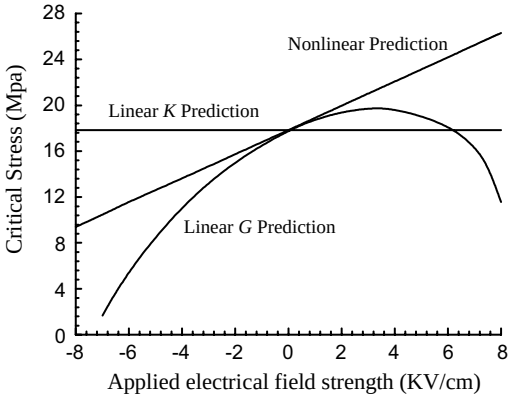

Fig. 3. Variations of fracture loads with applied electric field strengths (Half crack length is $a = 1$ mm).

factor and the energy release rate criteria, if the electrical non-linearity is taken into consideration. Accordingly, there is only one cave for non-linear prediction, which increases linearly with the applied electric field load. Conversely, predictions based on linear crack model are different for K criterion and G criterion. The electric field has no effect on the fracture load if linear K criterion is used. Further, for linear G criterion, the predicted fracture loads increase with applied electric field, to a peak value, and then decrease.

Fig. 4 shows the relationship between the critical applied stress and electric field intensity factors, based on the electrically non-linear model. The assumed fracture toughness in the absence of electric field is $K_{IC} = 1$ Mpa $\sqrt{\text{m}}$. It can be shown that the critical applied stress intensity factor is an increasing function of the critical electric field intensity factor. Hence, a positive electric field will improve and a negative electric field will decrease the fracture toughness of the piezoelectric media. The nonlinear prediction in Fig. 4 for PZT-PIC 151 material agree qualitatively with existing experimental observations made by Heyer et al. (1998). Such a fact suggests that the electric field non-linearity model proposed in this paper is reasonable for piezoelectric materials with conducting cracks. For comparison, Fig. 4 also plots the prediction based on the linear G criterion.

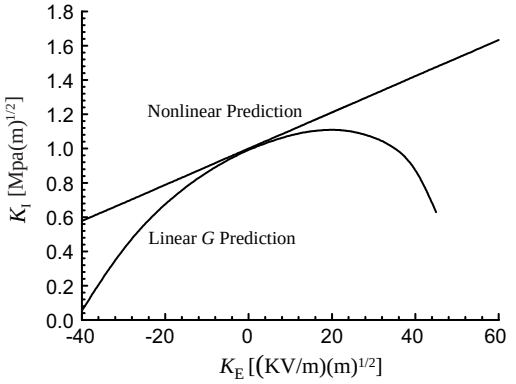

Fig. 4. Critical applied stress and electric field intensity factors for PZT-PIC 151 ($K_I = \sigma_\infty \sqrt{\pi a}$, $K_E = E_\infty \sqrt{\pi a}$).

6. Conclusion

An electric field based non-linear model for a conducting crack in piezoelectric materials is proposed. The model is analogously similar to the strip dielectric breakdown model proposed by Zhang and Gao (2004). The model requires only some basic material properties, such as the elastic constants, piezoelectric constants and dielectric permittivities. Expressions for stress intensity factor and energy release rate are obtained in closed-form and they do not depend on the electric field saturation strength of the media. It is found that crack propagation can either be enhanced or be retarded depending on the direction of the electric field. Theoretically predicated fracture loads based on the proposed model agree qualitatively with existing experimental observations.

Acknowledgements

The authors are very grateful to the anonymous reviewers for their valuable comments. BLW also thanks the Australia Research Council for their support through an ARC Discovery-Project Grant (#DP0346037) and an ARC Australian research fellowship.

References

Cooper, R., 1963. The electric strength of solid insulation. Int. J. Electrical Eng. Educat. 1, 241.
Estrada, R., Kanwal, R.P., 2000. Singular Integral Equations. Birkhäuser, Boston.
Fulton, Gao, 1997. Electrical nonlinearity in fracture of piezoelectric ceramics. App. Mech. Rev. 50 (11), part 2.
Gao, H.-J., Zhang, T.Y., Tong, P., 1997. Local and global energy release rates for an electrically yielded crack in a piezoelectric ceramic. J. Mech. Phys. Solids 45 (4), 491–510.
Heyer et al., 1998. A fracture criterion for conducting cracks in homogeneous poled piezoelectric PZT-PIC 151 ceramics. Acta Mater. 46 (18), 6615–6622.
Konda, N., Erdogan, F., 1994. The mixed mode crack problem in a nonhomogeneous elastic medium. Eng. Fract. Mech. 47, 533–545.
Kuffel, E., Zaengl, W.S., 1984. High-voltage Engineering: Fundamentals. Pergamon Press, Oxford, New York.
Park, S.B., Sun, C.T, 1995. Effect of electric field on fracture of piezoelectric ceramics. Int. J. Fract. 70, 203–216.
Ricoeur, A., Kuna, M., 2003. A micromechanical model for the fracture process zone in ferroelectrics. Computat. Mater. Sci. 27, 235–249.
Ru, C.Q., 1999. Effect of electrical polarization saturation on stress intensity factors in a piezoelectric ceramic. Int. J. Solids Struct. 36, 869–883.
Suo, Z., 1993. Models for breakdown-resistant dielectric and ferroelectric ceramics. J. Mech. Phys. Solids 41, 1155–1177.
Suo, Z., Kuo, C.-M., Barnett, D.M., Willis, J.R., 1992. Fracture mechanics for piezoelectric ceramics. J. Mech. Phys. Solids 40, 739–765.
Wang, T.C., 2000. Analysis of strip electric saturation model of crack problem in piezoelectric materials. Int. J. Solids Struct. 37, 6031–6049.
Winzer, S.R., Shankar, N., Ritter, A., 1989. Designing cofired multilayer electrostrictive actuators for reliability. J. Am. Ceram. Soc. 72, 2246–2257.
Yang, W., Zhu, T., 1998. Switch-toughening of ferroelectrics subjected to electric fields. J. Mech. Phys. Solids 46, 291–311.
Zeller, H.R., Schneider, W.R., 1984. Electrofracture mechanics of dielectric aging. J. Appl. Phys. 56, 455–459.
Zhang, T.Y., Gao, C.F., 2004. Fracture behavior of piezoelectric materials. Theoretical and Applied Fracture Mechanics 41 (1–3), 339–379.
Zhang, T.Y., Wang, T.H., Zhao, M.H., 2003. Failure behavior and failure criterion of conductive cracks (deep notches) in thermally depoled PZT-4 ceramics, 51 (16) 4881–4895.